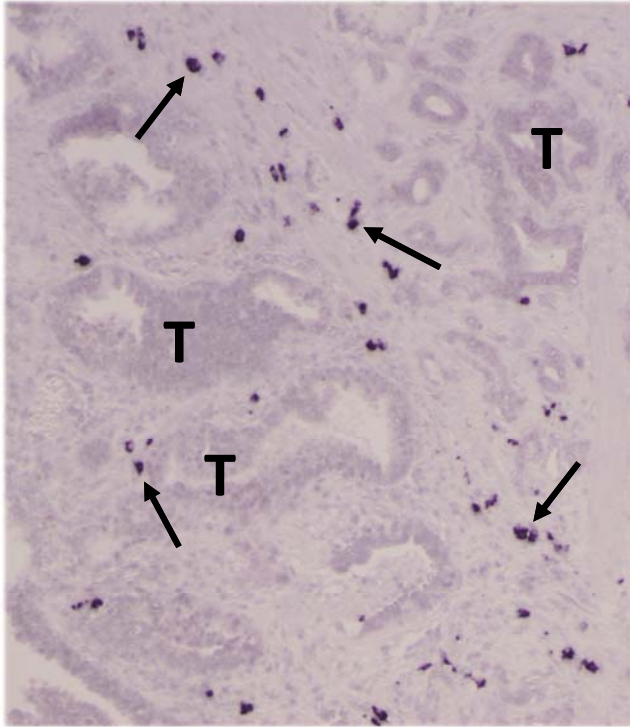
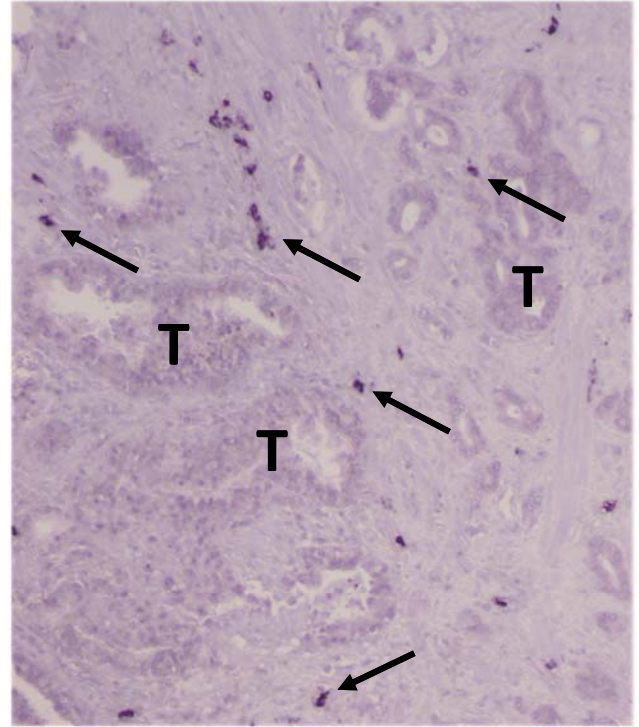


Supplementary Figure S1: Weight curves for untreated TRAMP mice and TRAMP mice treated with nicotine for 80 days. Weight of animals treated with nicotine was 10% to 20% lower than the weight of untreated animals at day 80 ($P < 0.05$, ANOVA and post-hoc t-test).

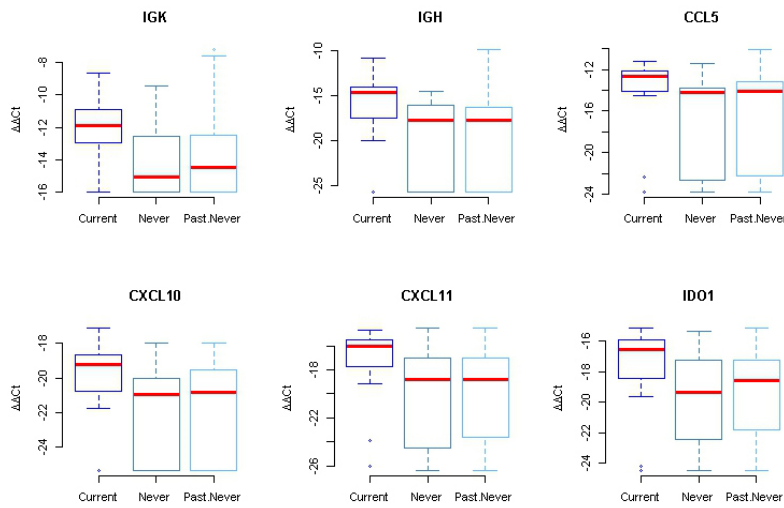
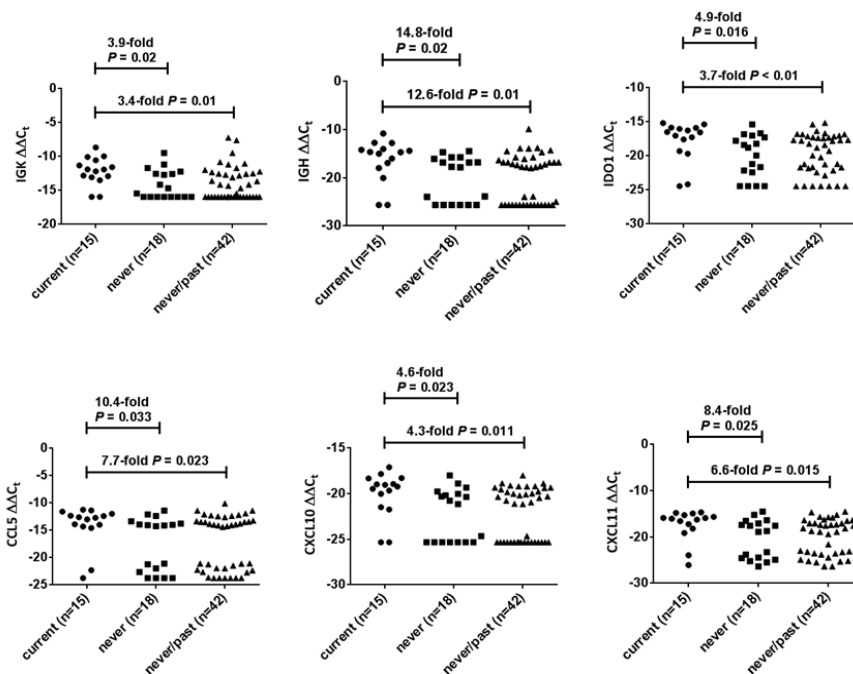
Kappa light chain ISH



Lambda light chain ISH

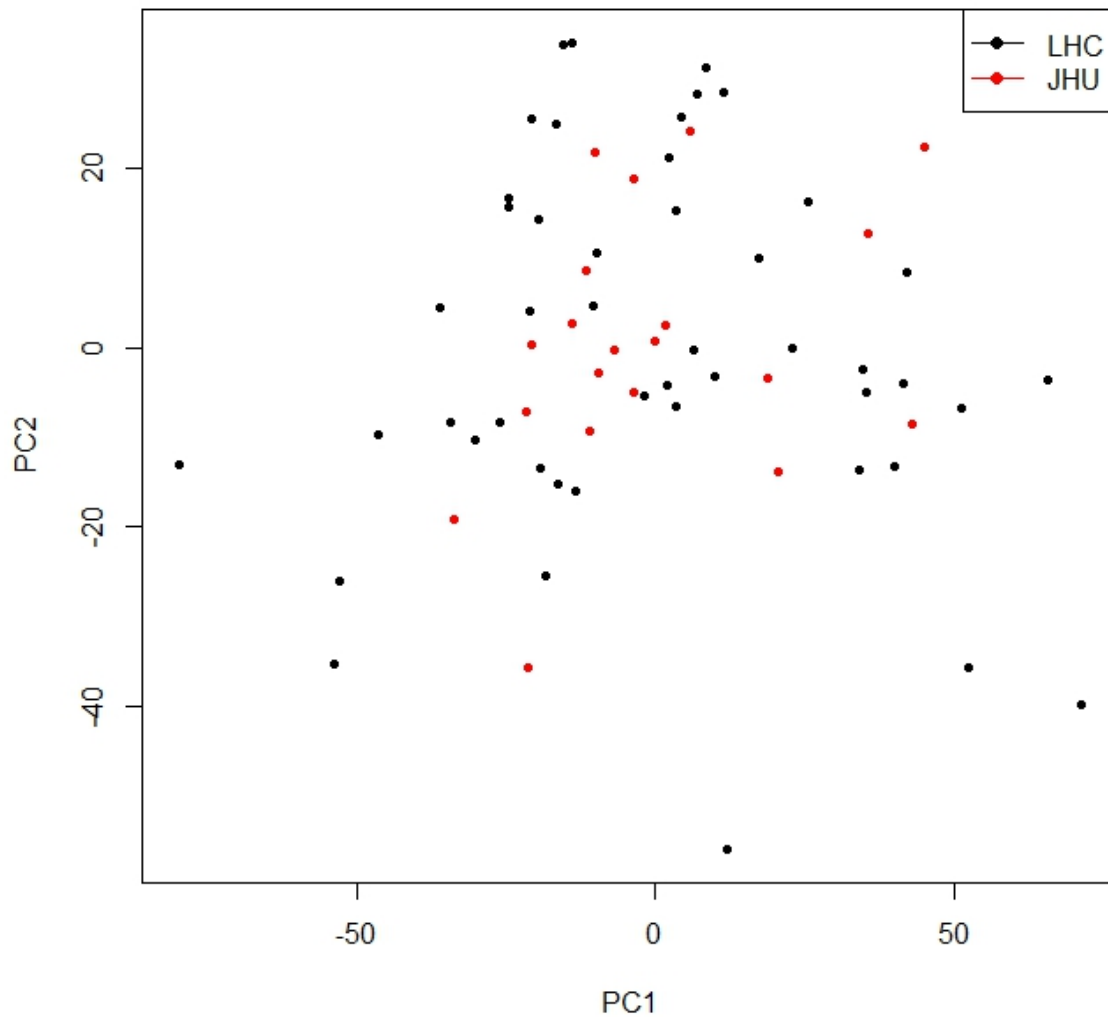


Supplementary Figure S2: Ig lambda- and Ig kappa-positive B lymphocytes in cancerous prostate tissue by in-situ hybridization. Ig lambda- and Ig kappa-positive B lymphocytes were visualized by in-situ hybridization (ISH) as described under methods. Accumulation of the dark blue nitroblue tetrazolium chromogene (see arrows) reveals the stromal localization of immunoglobulin (mRNA)-positive B lymphocytes. Arrows depict kappa and lambda light chain-positive cells in stroma adjacent to tumor tissue (T).

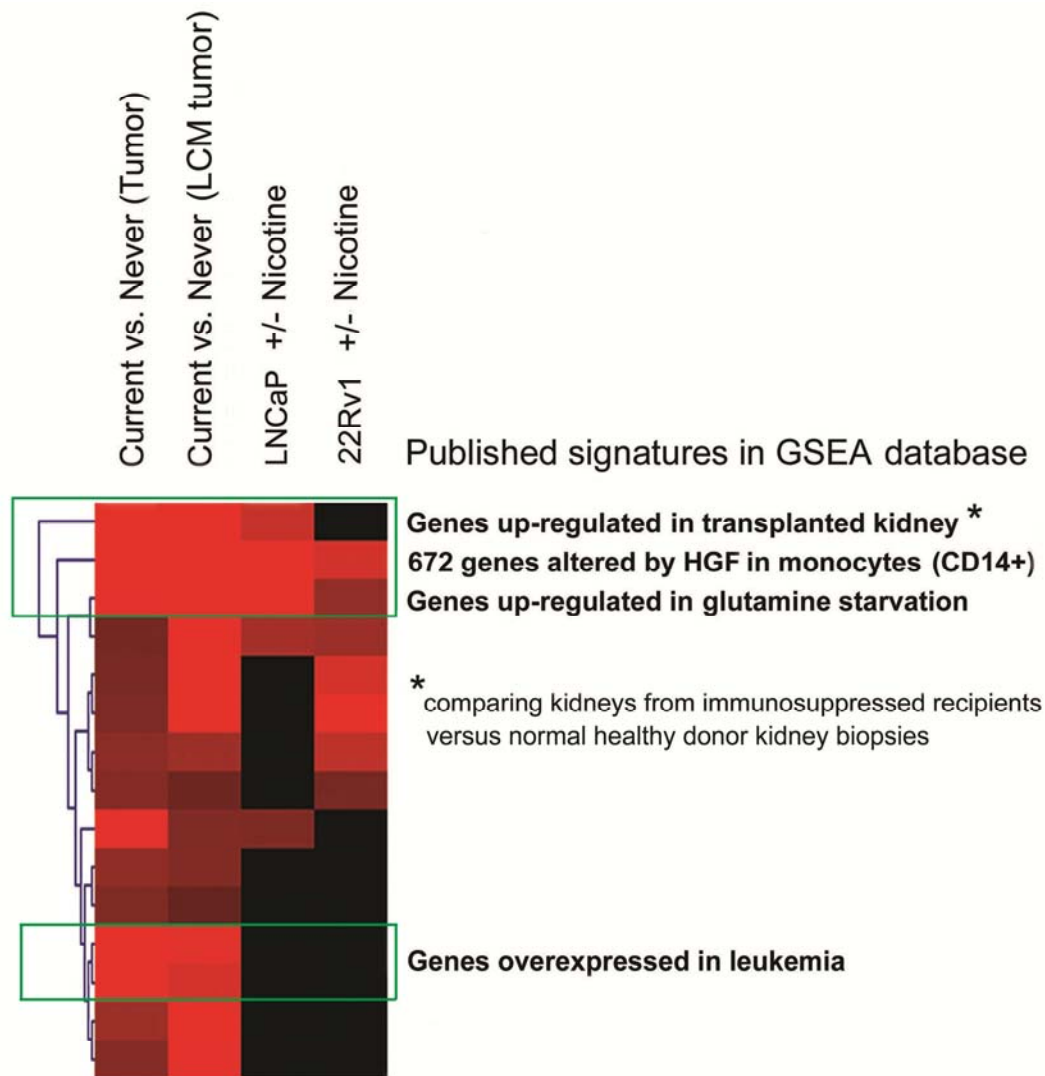
A**B**

Supplementary Figure S3: qRT-PCR validation of six genes up-regulated among current smokers. qRT-PCR was performed with RNA from 57 tumors (15 current, 18 never, 24 past smokers) previously analyzed by gene microarray. **A.** Boxplots show expression patterns for 6 genes among current, never, and past/never smokers. Expression differences between current smokers and never or past/never smokers are significant for all 6 genes (Kruskal-Wallis test; $P < 0.05$). Bars in figures show median expression. **B.** Same graphs as scatterplots highlight low expression of these immune genes in many tumors from never or past smokers. Fold difference was derived from $2^{-\Delta\Delta C_t}$ values (see Methods).

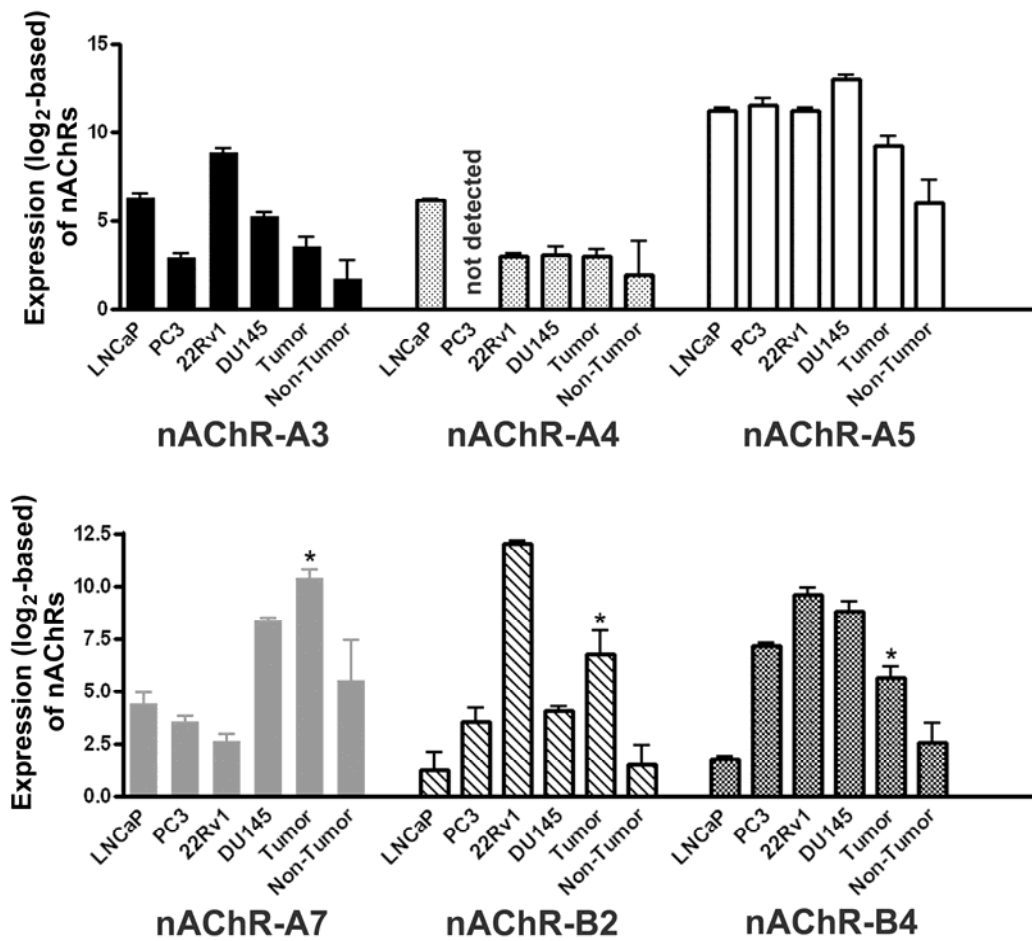
ComBat combine LHC and JHU



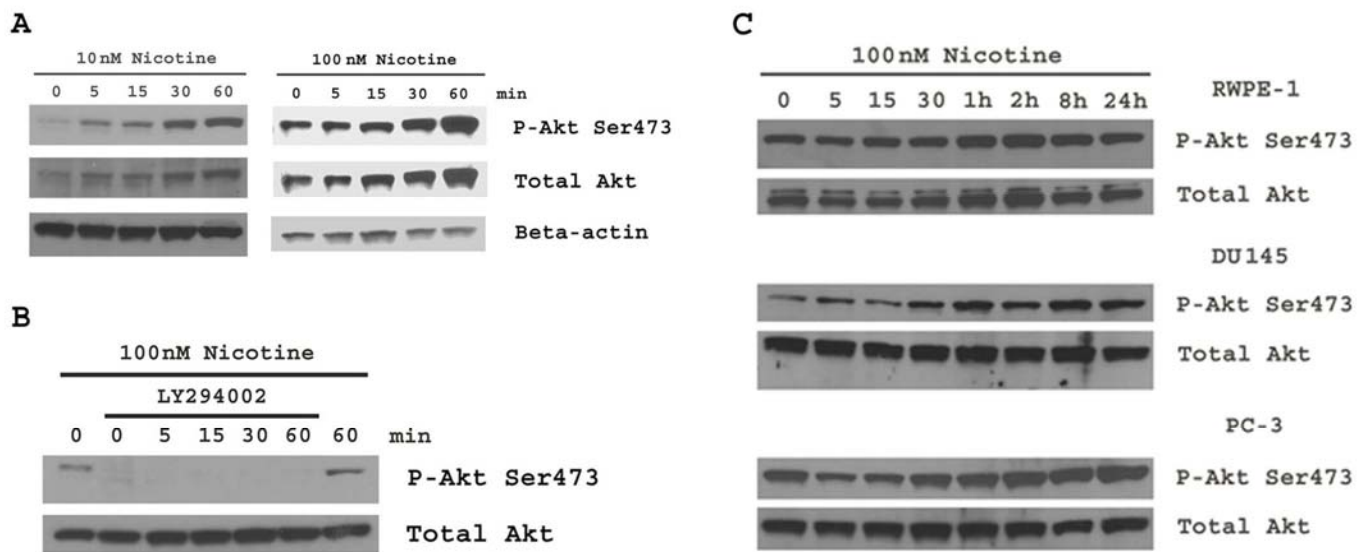
Supplementary Figure S4: Analysis of prostate tumors using Bioconductor limma R. Here, a possible batch effect for the two datasets ("LHC" and "JHU") was corrected with ComBat. PCA plot shows the absence of a batch effect between the discovery dataset "LHC" (n=47) and the "JHU" dataset (n=20) after applying ComBat, an R package using an empirical Bayes method to remove batch effects (<http://www.bu.edu/jlab/wp-assets/ComBat/Abstract.html>).



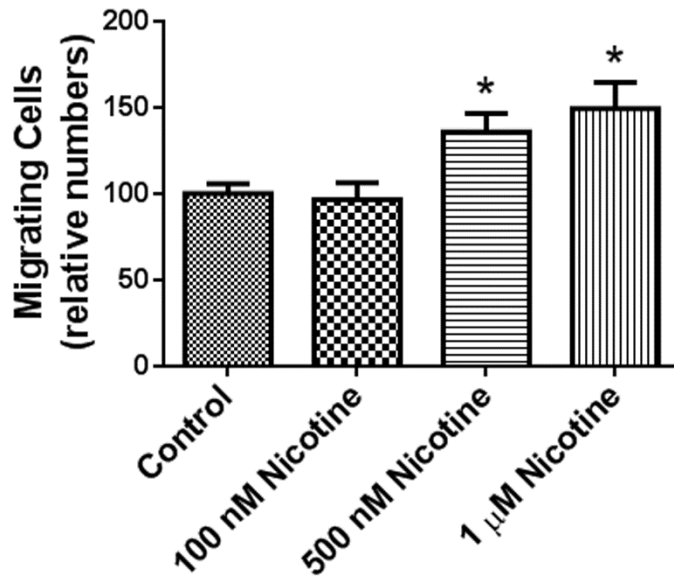
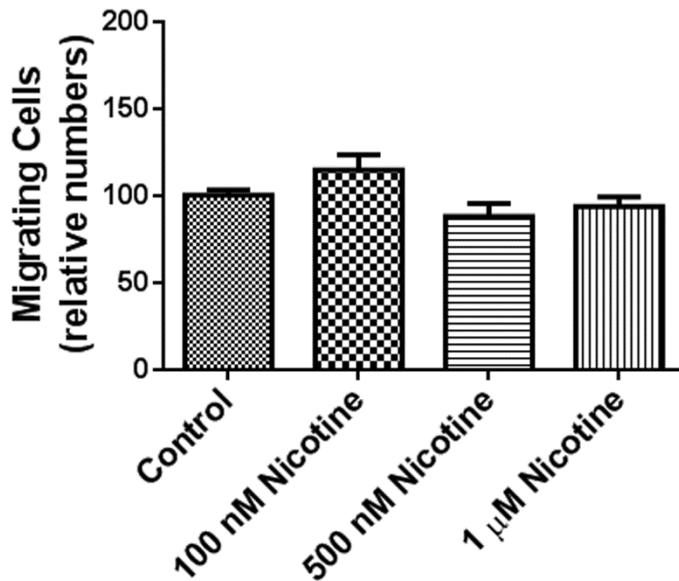
Supplementary Figure S5: Gene Set Enrichment Analysis (GSEA) highlighting common features between smoking-related gene signatures in prostate tumors, nicotine-induced gene signatures in human prostate cancer cells, and gene signatures archived in the GSEA database. The color coding (intensity of red) depicts an association in the gene expression pattern between datasets archived in the GSEA database (<http://www.broad.mit.edu/gsea/msigdb>) and gene lists from our study (e.g., current vs. never smokers in tumor), with an increased red intensity indicating a higher enrichment score and a stronger association ($-\text{Log}(P \text{ value})$ -based). Shown is a heatmap of a cluster analysis to illustrate associations between the smoking-related gene signatures in macrodissected (Tumor) and microdissected (LCM tumor) prostate tumors and previously identified gene signatures (e.g., a hepatocyte growth factor-induced gene signature in CD14-positive monocytes). Shown is also the association of these published signatures with nicotine-induced gene signatures in LNCaP and 22Rv1 human prostate cancer cells. LNCaP and 22Rv1 cells were treated with 100 nM nicotine/solvent for 24 hours ($n = 6$ per treatment). Green frames highlight GSEA terms that are significantly associated with the smoking-related gene signature in both macrodissected and microdissected prostate tumors.



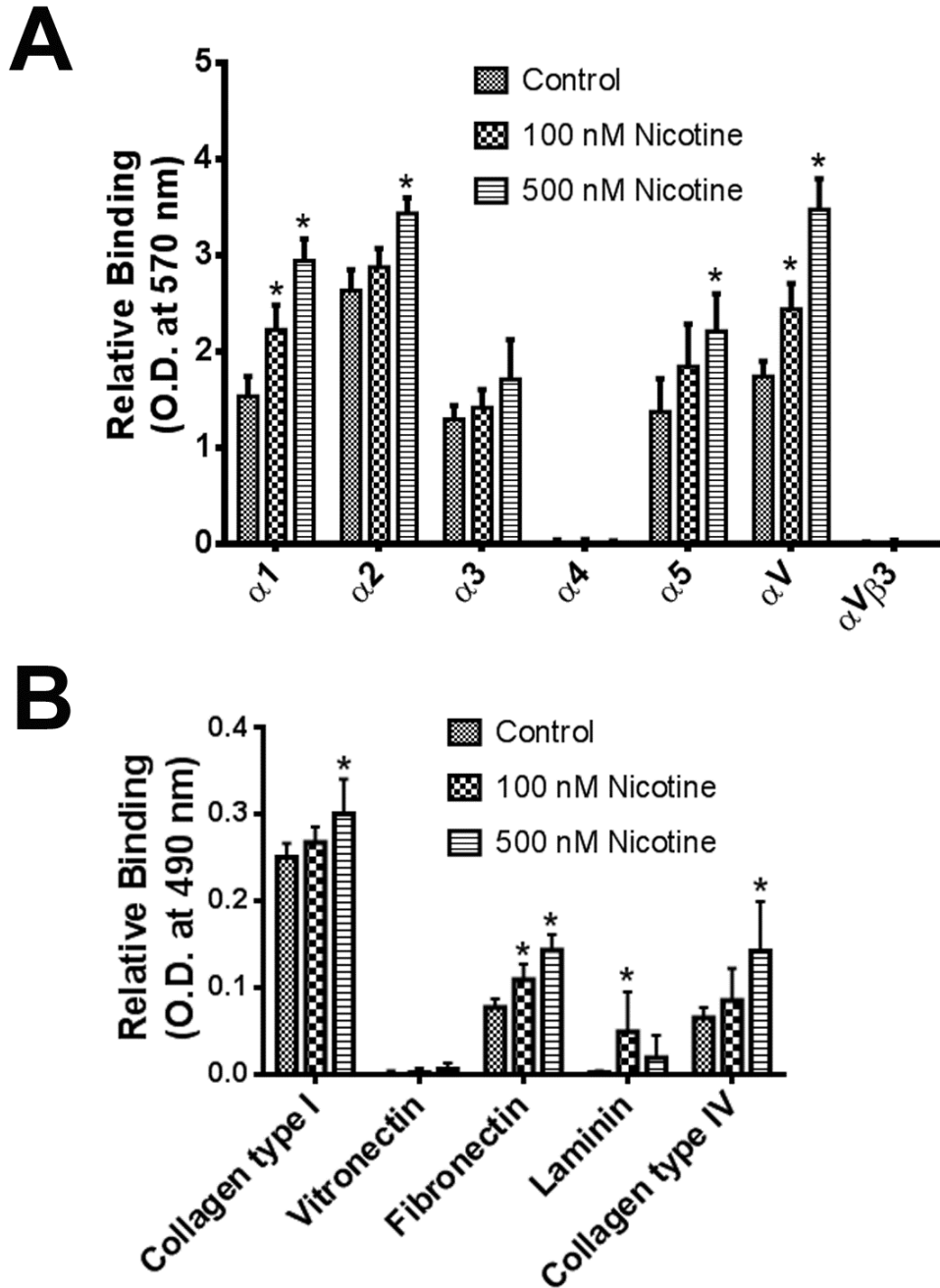
Supplementary Figure S6: Expression of various nicotinic acetylcholine receptor (AChR) subunits in human prostate cancer cell lines, prostate tumors, and adjacent non-tumor prostate tissues. qRT-PCR analysis of mRNA abundance for AChRs and 18s ribosomal RNA. Shown is the relative expression of the receptors calculated as relative C_t value (18s-nAChR). Mean \pm SD; triplicate measurements for cell lines; n = 4 for tumor and adjacent non-tumor tissues, respectively. *Expression of nAChR- α 7, β 2, and β 4 subunits was significantly increased in tumors when compared with adjacent non-tumor tissue ($P < 0.05$, t-test).



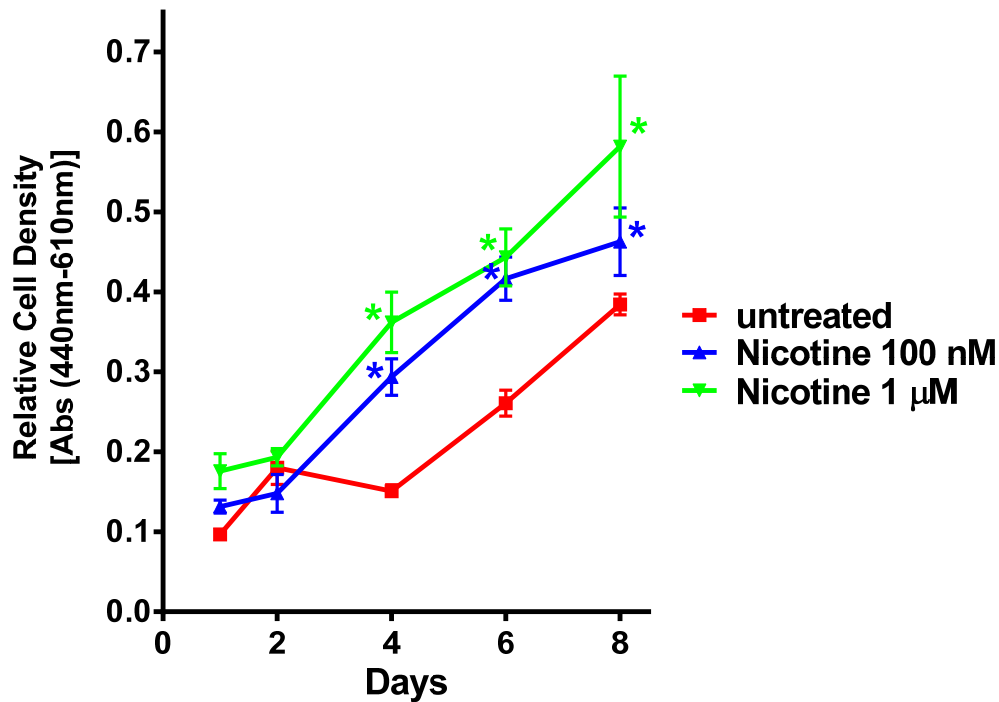
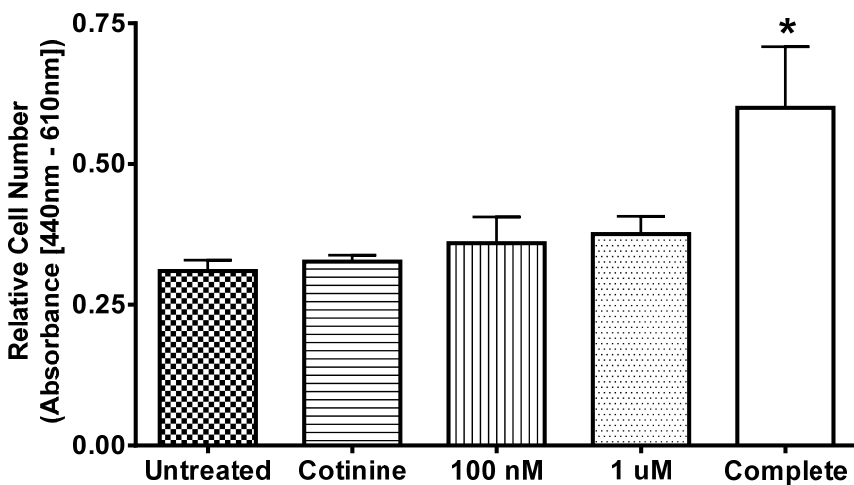
Supplementary Figure S7: Nicotine-mediated Akt activation in human immortalized prostate epithelial cells and prostate cancer cell lines. Nicotine at 10 nM and 100 nM concentrations induced Akt phosphorylation in RWPE-1 immortalized human prostate epithelial cells (**A**). LY294002 (10 μ M), a PI3 kinase inhibitor, abrogated nicotine-induced phosphorylation of Akt in these cells (**B**). Time course of Akt phosphorylation over a 24-hour time period in RWPE-1 cells and in DU145 and PC-3 prostate cancer cell lines (**C**).

A**B**

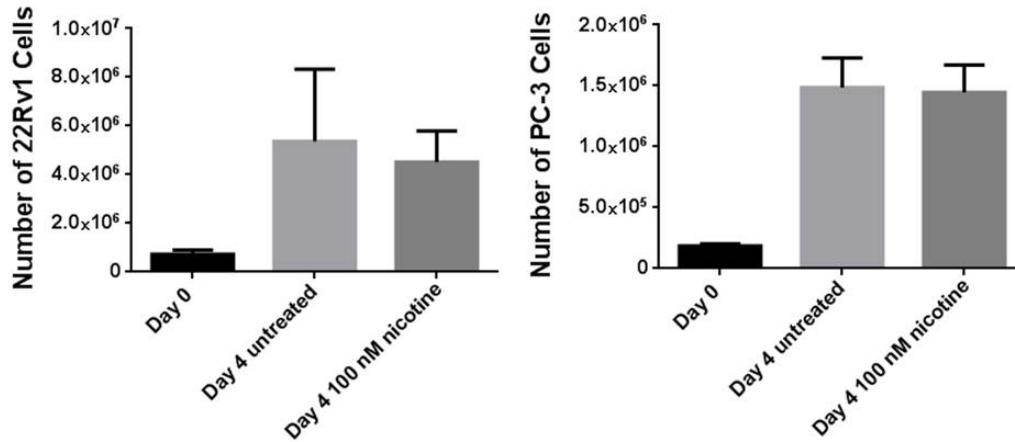
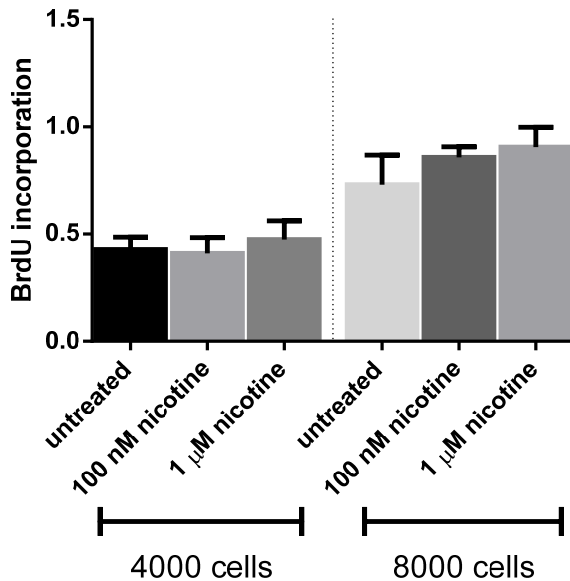
Supplementary Figure S8: Effect of nicotine on the mobility of human prostate cancer cell lines. 22Rv1 (A) and PC-3 (B) cells were treated with three nicotine concentrations. Only at the higher concentrations, it significantly increased mobility of 22Rv1 cells (A). Cells were plated into the BD Biosciences HTS multiwell insert system (1×10^5 cells each) and cells were treated with 100 nM, 500 nM, and 1 μM nicotine. After 24 hours, the number of cells that migrated to the outer side of the insert were determined by counting cell numbers in 5 fields per well at 200x magnification. Numbers of migrating cells are reported as the average number of migrating cells over 3 wells. Mean \pm SD; triplicate measurements for cell lines. *significantly different from control ($P < 0.05$).



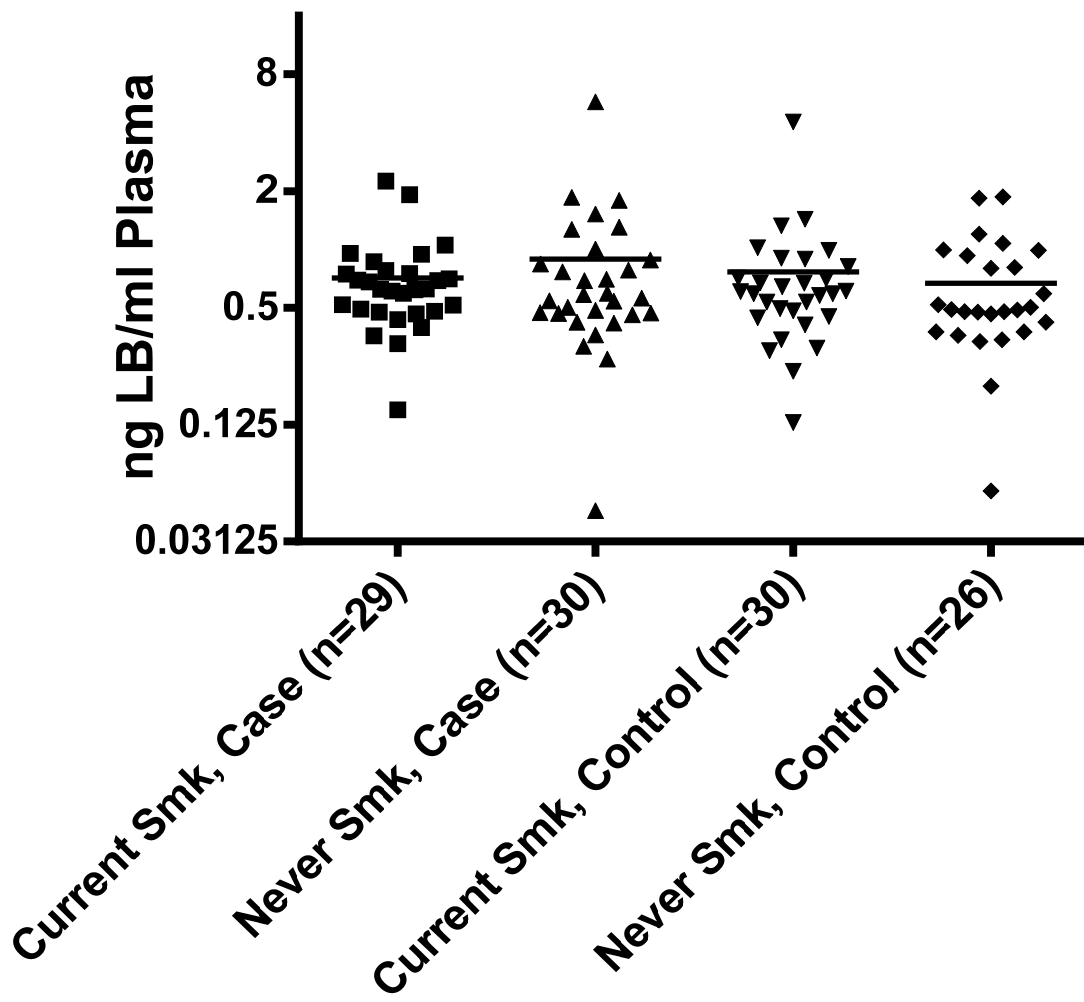
Supplementary Figure S9: Nicotine enhances cell surface integrin expression and extracellular matrix binding (ECM) of 22Rv1 human prostate cancer cells. Shown is (A) increased integrin subunit expression and (B) ECM binding of nicotine-treated 22Rv1 cells. Cells were treated with nicotine for 24 hours and then plated onto (A) antibody-coated wells to capture integrin expressing cells or (B) wells pre-coated with fibronectin, vitronectin, laminin, collagen I or collagen IV. Binding of cells to these ECM surfaces was measured as described under methods. Mean \pm SD; triplicate measurements in A, n = 5-7 in B. *significantly different from control ($P < 0.05$).

A**B**

Supplementary Figure S10: Nicotine enhances proliferation of RWPE-1 in complete K-SFM medium but not in K-SFM medium without EGF and bovine pituitary extract. (A) RWPE-1 cells were cultured in K-SFM medium and treated with nicotine (100 nM and 1 µM) for 8 days. (B) RWPE-1 cells were treated with cotinine (2.5 µM) or nicotine (100 nM and 1 µM) for 5 days in growth factor-depleted K-SFM medium. For comparison, cells were cultured in complete K-SFM medium. Cell proliferation was measured in 96-well plates using the WST-1 assay. Cells were plated at day zero at 5000 cells/well. Mean ± SD; triplicate measurements for cell lines. * $P < 0.05$, vs. control (ANOVA test).

A**B**

Supplementary Figure S11: Nicotine did not enhance proliferation of 22Rv1 and PC-3 human prostate cancer cells. **A.** 22Rv1 and PC-3 cells were exposed to 100 nM nicotine for 4 days and average cell numbers were determined using a Bio-Rad TC10 Automated Cell Counter. **B.** Incorporation of BrdU into nicotine-treated 22Rv1 cells seeded at two different cell densities in 96-well plates. BrdU incorporation was measured by ELISA 24 hrs after treatment with nicotine. Triplicate measurements (A) or $n = 4$ (B). Shown is mean \pm SD. Significant differences between treated and untreated were not observed.



Supplementary Figure S12: Lymphotoxin- β plasma levels in prostate cancer patients (Case) and population-based controls (Control) by smoking status. Lymphotoxin- β (LB) plasma levels were not associated with the smoking status in prostate cancer patients or controls. No significant differences between groups: $P = 0.68$, ANOVA test. Plasma LB concentrations were determined using an ELISA test (at a NCI core facility).